AIP | Journal of Applied Physics

Transient thermal and nonthermal electron and phonon relaxation after short-pulsed laser heating of metals

Ashutosh Giri and Patrick E. Hopkins

Citation: Journal of Applied Physics **118**, 215101 (2015); doi: 10.1063/1.4936606
View online: http://dx.doi.org/10.1063/1.4936606
View Table of Contents: http://scitation.aip.org/content/aip/journal/jap/118/21?ver=pdfcov
Published by the AIP Publishing

Transient thermal and nonthermal electron and phonon relaxation after short-pulsed laser heating of metals

Ashutosh Giri and Patrick E. Hopkins[a)]
Department of Mechanical and Aerospace Engineering, University of Virginia, Charlottesville, Virginia 22904, USA

(Received 16 August 2015; accepted 14 November 2015; published online 7 December 2015)

Several dynamic thermal and nonthermal scattering processes affect ultrafast heat transfer in metals after short-pulsed laser heating. Even with decades of measurements of electron-phonon relaxation, the role of thermal vs. nonthermal electron and phonon scattering on overall electron energy transfer to the phonons remains unclear. In this work, we derive an analytical expression for the electron-phonon coupling factor in a metal that includes contributions from equilibrium and nonequilibrium distributions of electrons. While the contribution from the nonthermal electrons to electron-phonon coupling is non-negligible, the increase in the electron relaxation rates with increasing laser fluence measured by thermoreflectance techniques cannot be accounted for by only considering electron-phonon relaxations. We conclude that electron-electron scattering along with electron-phonon scattering have to be considered simultaneously to correctly predict the transient nature of electron relaxation during and after short-pulsed heating of metals at elevated electron temperatures. Furthermore, for high electron temperature perturbations achieved at high absorbed laser fluences, we show good agreement between our model, which accounts for d-band excitations, and previous experimental data. Our model can be extended to other free electron metals with the knowledge of the density of states of electrons in the metals and considering electronic excitations from non-Fermi surface states. © *2015 AIP Publishing LLC*. [http://dx.doi.org/10.1063/1.4936606]

I. INTRODUCTION

The relaxation and scattering mechanisms within and between the fundamental energy carriers in solids is a critical parameter in thermal management and design of micro- and nanoscale devices. As length and time scales decrease and device power densities increase, electron scattering mechanisms become the increasingly dominant resistance to thermal transport in these devices.[1] These scattering events can lead to hot spots and device heating, and thus must be better understood to properly design next-generation devices.

In this regard, pump-probe, short-pulsed thermoreflectance techniques have proven to be reliable in measuring the temporal evolution of electronic relaxation and scattering mechanisms, including Fermi relaxation of a perturbed electron gas,[2–4] the electron-phonon (e-p) coupling factor,[5–7] and electron-interface scattering.[8,9] In a typical short-pulsed-based pump-probe experiment to measure the ultrafast electron relaxation dynamics, the electrons are perturbed to a non-Fermi distribution by a pump pulse that is focused on the sample surface. A time delayed probe pulse monitors the subsequent relaxation of the electron gas into a near-Fermi distribution followed by the relatively longer e-p thermalization process. The change in the reflectivity of the probe pulse (the thermoreflectance response) is related to the electron relaxation and scattering mechanisms.[10,11]

The difficulty in pump-probe thermoreflectance experiments, however, is in the interpretation of the measured transient energy transfer processes. The conventional and most widely applied method is to compare the experimental data to the well known Two Temperature Model (TTM)[12] by fitting the TTM to the experimentally measured temporal decay in reflectivity to determine e-p coupling factor, G. It should be noted that the experimental results could also be compared to more rigorous models that are based on the density functional theory[13–15] and molecular dynamics in conjunction with the TTM[16,17] to predict the electron dynamics. However, these aforementioned models often inherently assume that the electronic states can be defined by a finite temperature, whereas, photoemission and pump-probe femtosecond measurements have demonstrated a long-living non-Fermi distribution of electrons in gold (that can take as long as ~1 ps to thermalize, depending on the laser fluence and wavelength).[2,4,18,19] Due to the ultrafast excitation from laser pulses with pulse widths shorter than the time taken by the electrons to relax to a Fermi distribution, this assumption of a completely thermalized electronic system is rendered invalid.[20–22] Along with the assumption of a thermalized electron system, the TTM approach also assumes that the measured G is constant during the entire relaxation time probed by the experiment. This assumption is questionable as experiments have demonstrated an almost two-fold increase in G, resulting from high absorbed laser fluences that perturb the electronic states to temperatures of thousands of degrees above ambient condition.[4,7,9,10,23] In this regard, the assumption of a constant G is not entirely valid as various scattering mechanisms contribute to the increase in the transient relaxation measured during pump-probe experiments at elevated electron temperatures, T_e. Therefore, even with decades of short-pulsed e-p coupling measurements, the following fundamental questions remain:

a)Electronic mail: phopkins@virginia.edu

- What processes contribute most significantly to the overall rate of energy transfer from an excited electron system to the lattice: electron-electron (e-e) scattering or e-p scattering?
- Additionally, how do the nonthermal vs. thermal states of the electron system affect e-p equilibration?

We seek to answer these questions in this work.

Chen *et al.*[24] predicted a linear trend in G with electron and phonon temperatures during e-p nonequilibrium, given as

$$G = \frac{\pi^2 m v_s^2 n_e}{6}[A_{ee}(T_e + T_p) + B_{ep}], \tag{1}$$

where m is the free electron mass, v_s is the sound velocity, n_e is the free electron number density, T_p is the phonon temperature, and A_{ee} and B_{ep} are the e-e and e-p scattering coefficients, respectively. This expression for G was derived from the expression of Kaganov *et al.*[25] for the e-p coupling factor, which is only valid for free electron metals with relatively constant density of states (DOS), but extends the model of Kaganov *et al.* to nonequilibrium situations in which $T_e > T_p > T_D$, where T_D is the Debye temperature of the solid. The temperature trend in Eq. (1) comes from the assumption that e-e scattering of a thermalized electron gas affects e-p scattering, and hence G.

More recently, Lin *et al.*[26] re-derived the temperature dependence of the e-p coupling factor for several metals using an *ab initio* density of states for electrons. This approach did not account for e-e relaxation, as the work questioned the validity of accounting for e-e scattering while calculating strictly e-p interactions. Their calculations were based on the e-p coupling factor derived by Allen,[27] which is not limited to free electron metals with a relatively flat density of states but is applicable to metals with arbitrary density of states, that is given by

$$G = -\frac{\pi\hbar k_B \lambda\langle\omega^2\rangle}{g(\epsilon_F)}\int g^2(\epsilon)\frac{\partial f(\epsilon)}{\partial\epsilon}d\epsilon, \tag{2}$$

where $\hbar$ is the reduced Plank's constant, k_B is the Boltzmann constant, λ is the e-p mass enhancement parameter, $\langle\omega^2\rangle$ is the second moment of the phonon spectrum, and $g(\epsilon)$ is the density of states of the electronic system. This general form of the e-p coupling factor in a metal is applicable for high temperatures where electronic states away from the Fermi surface have to be considered for calculations of the temperature dependency of G. It should be noted that Eq. (2) assumes fully thermalized electron and phonon systems and e-e interactions do not affect the e-p energy transfer process.

The two theories described in the previous paragraphs (the Chen *et al.*[24] theory for free electron metals and Allen's[27] theory for any metal) predict two different e-p coupling factors when the electron and phonon ensembles are out of equilibrium. Furthermore, both theories assume that the electrons can be described by a Fermi distribution and do not take into account nonthermal electron to phonon coupling. Therefore, this warrants further investigation into the temperature dependency of G, including the scenario where the electrons are temporarily out of equilibrium with the surrounding lattice and/or in a nonthermal distribution after short-pulsed excitation. Several experimental works have investigated the temperature dependence of G using the aforementioned pump-probe thermoreflectance technique.[3,7–9,23] However, these studies predict (and assume) a constant G (by varying the incident pump fluence and fitting the experimental data with the TTM) for the time period considered in the experiment and neglect the temperature dependency of G during this time period when the "hot" electrons are losing energy to the phonons. Along with that, various works have also alluded that nonthermal electron to phonon coupling can present a significant channel for electronic energy relaxation in metals.[21,22,28,29]

In this work, we investigate the various scattering mechanisms that influence e-p energy relaxation processes in metals. In Section II, we derive an analytical expression for the e-p relaxation rate that accounts for energy exchange to the lattice from an electron system that cannot be described by an equilibrium distribution or a temperature. We conduct example calculations for Au, a well-studied free-electron metal, but our approach can be extended to metals with an arbitrary density of states. In Section III, we investigate the validity of the various models for G in predicting the thermoreflectance response of a Au film during and after short-pulse absorption at high and low fluences. Our results demonstrate that only accounting for e-p scattering (considering both thermalized and/or nonthermal electron distributions) in the e-p coupling factor under-predicts the energy relaxation rates measured during and after high laser pulse absorption; in these experimental situations, to properly account for the total energy transfer from the electronic to phononic systems, e-e scattering must be considered. In Section IV, we derive the equation of electron energy transfer (EEET) with a relaxation time approximation (RTA), which describes the change in electron internal energy as a function of time due to e-p scattering; we also re-derive Allen's expression for an arbitrary density of states and recast this expression into an electron internal energy balance in line with the EEET. From these results, we determine the transient e-p coupling factor during hot electron relaxation after short-pulsed absorption given a temperature profile as a function of time. Finally, we extend Chen's model for the electron-phonon coupling factor to high temperatures where d-band excitations dominate the relaxation process, and show better agreement between experimental data and the modified Chen model compared to previous Chen *et al.*[24] and Allen[27] models. Although we report specific results for gold, the method and model we derive are valid for any free electron metal. We summarize our results in Section V.

II. NONTHERMAL ELECTRON DYNAMICS

Consider an electron system that is perturbed from its equilibrium distribution. The electronic distribution is divided into thermal and nonthermal parts

$$f(\epsilon) = \left(n_{ex}\exp\left[-\frac{t}{\tau_{ee}}\right]\right)f_0(\epsilon, T) + f_{FD}(\epsilon, T_e), \tag{3}$$

where n_{ex} is the percentage of electrons excited into a nonthermal distribution state, t is the time after excitation, and f_{FD} represents the equilibrium, or Fermi Dirac distribution function, τ_{ee} is the quasiparticle lifetime of an electron with energy $\delta\epsilon = \epsilon - \epsilon_F$ above the Fermi energy interacting with electrons in a Fermi distribution, and f_0 is the nascent electron distribution immediately after excitation (i.e., laser pulse absorption).[18] This serves as an initial condition for the nonthermal part of the electronic distribution and extends from the Fermi energy to the laser photon energy above the Fermi energy. Also, due to the fact that a temperature cannot be explicitly described for a perturbed electron distribution, we assume that the nascent distribution can be described by the ambient temperature, T. Assuming $\delta\epsilon \gg k_B T_e$, which is typical after ultrashort-pulsed laser absorption, this nonthermal electron lifetime is given by the Fermi-liquid theory[30]

$$\frac{1}{\tau_{ee}} = \frac{\pi^2\sqrt{3}\omega_p}{128}\left(\frac{\delta\epsilon}{\epsilon_F}\right)^2, \tag{4}$$

where ω_p is the plasma frequency. Equation (4) suggests that the higher the energy of the particle, the faster the relaxation time. This has been demonstrated experimentally by Fann *et al.*[18] using time-resolved photoemission spectroscopy to measure the electron energy distribution after short-pulsed irradiation of Au films. In Fig. 1, we plot the calculations of Eq. (3) for the laser fluences and wavelengths used in Ref. 18 to perturb the electron distribution in Au. These calculations agree with the experimental results in Ref. 18, where they show that for the lower absorbed fluence case (Fig. 1(a)), the nonthermal distribution is still prominent even at times of 670 fs after laser pulse absorption. However, the thermalization time decreases for the higher fluence case due to the increased number of excited electrons.

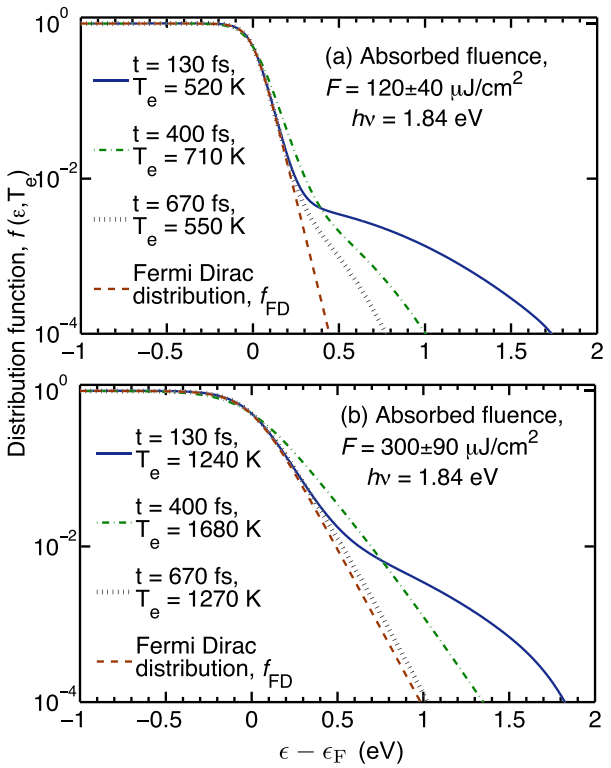

FIG. 1. Electron energy distribution functions vs. energy calculated via Eq. (3) for Au after short-pulse laser heating fluences of (a) 120 μJ/cm^2 and (b) 300 μJ/cm^2 as experimentally investigated in Ref. 4. Overall, the form of the distribution function described by Eq. (3) exhibits good agreement with the previously published experimental data.[4]

Inserting the generalized electronic distribution into Eq. (2) yields the generalized e-p coupling factor in a metal when the electrons have not relaxed into an equilibrium Fermi-Dirac distribution given by

$$G(t) = -\frac{\pi\hbar k_B \lambda\langle\omega^2\rangle}{g(\epsilon_F)}\left(\int_{-\infty}^{\infty} g^2(\epsilon)\frac{\partial f_{FD}}{\partial\epsilon}d\epsilon + \int_{\epsilon_F}^{\epsilon_F+\delta\epsilon} g^2(\epsilon)\frac{\partial f_0}{\partial\epsilon}n_{ex}\exp\left[-\frac{t}{\tau_{ee}}\right]d\epsilon\right). \tag{5}$$

This equation allows for an assessment of the relative roles of thermal vs. nonthermal electronic distributions on e-p energy exchange via comparisons with Eq. (2). Note that Eq. (5) is a function of time after electronic excitation. The first integral term in Eq. (5) represents the e-p coupling factor, assuming a fully thermalized distribution of electrons at temperature T_e, while the second integral term represents the coupling from electrons in a nonthermal distribution to the phonons that after some time $t \gg \tau_{ee}$ relax into a thermal distribution. These nonthermalized electrons are also scattering with other electrons and relaxing into an equilibrium distribution while transferring energy to the lattice. Note that when the second term is thermalized, $\delta\epsilon \approx k_B T_e$ and Eq. (5) relaxes to Eq. (2). Also, if the electronic excitation $\delta\epsilon$ is less than or of the same order as $k_B T_e$, Eq. (5) simplifies to Eq. (2).

Figure 2 shows calculations of Eq. (5) for Au for three different excitation energies and two different electron temperatures

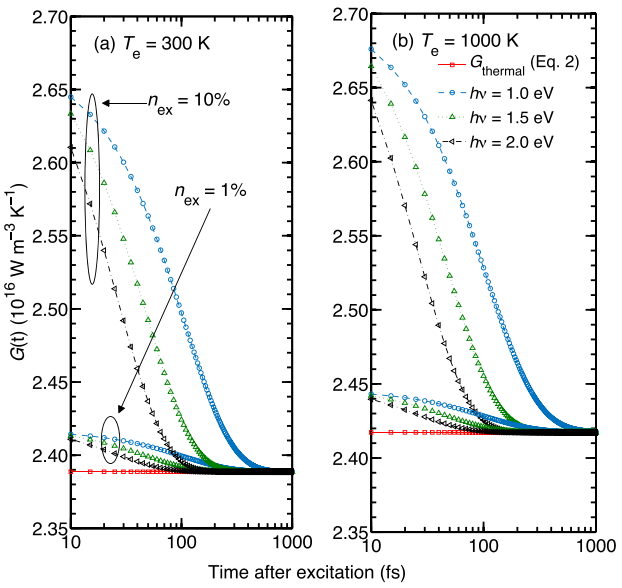

FIG. 2. Electron-phonon coupling factor, G, in Au as a function of time after excitation calculated via Eq. (5) for three different excitation energies, $h\nu = 1.0$, 1.5, and 2.0 eV, and two different electron temperatures, $T_e = 300$ (a) and 1000 K (b). The nonthermalized electrons do not interact with the phonons as frequently as the thermalized electrons, however, at relatively high excited electron densities, nonthermal electrons losing energy to the lattice can significantly increase G. Note also that this nonthermal electron effect on G lasts several hundred femtoseconds to a picosecond after excitation, depending on the excitation energy and the percentage of excited electrons, n_{ex}.

at 1% and 10% excited electron densities. The other properties of Au are taken from the free electron properties tabulated in the literature.[31] The calculations in this work assume no thermal or optical excitations from the $5d^{10}$ band in Au. The nonthermalized electrons in Au interact with the thermalized phonons, and cause a slight increase in G from that assuming a fully thermalized distribution. This increase in G increases with the number of electrons that are initially perturbed immediately following laser pulse excitation. This increase can be more than 10% at times, immediately following excitation when 10% of the conduction band electrons are perturbed to a nonthermal distribution. Although the nonthermalized portion can transfer a considerable amount of energy to the lattice, the increase in the e-p coupling predicted by Eq. (5) cannot explain the increase in relaxation rates observed for high electron temperature perturbations measured in transient thermoreflectance measurements.[4,7,23,32] This suggests that the additional rate of energy transfer from an excited electron system to the phonons, beyond that predicted from a fully thermalized e-p coupling factor, cannot be ascribed to any direct electron (thermal or nonthermal) to phonon interaction. Therefore, to understand the competing effects of different scattering mechanisms on e-p coupling in metals, we compare the validity of the various models described above in predicting the thermoreflectance response of Au under short-pulse laser excitation.

III. PUMP-PROBE THERMOREFLECTANCE MEASUREMENTS

We use a standard sub-picosecond pump-probe time domain thermoreflectance (TDTR) experiment to measure the transient relaxation of hot electrons in Au after pulsed laser absorption. Our pump-probe technique utilizes a two-wavelength approach where the pump pulses have been frequency doubled from 1.55 to 3.1 eV. The details of the experimental setup can be found in Refs. 33–35. The pump and probe pulses are focused on the surface of the sample, and the thermoreflectance signal from the reflected probe pulse is monitored with a photodiode that is locked into the modulation frequency of the pump heating event. In this work, we fix the pump modulation frequency to 8.8 MHz, and the cross-correlation of the pump and probe pulses at the sample surface is 780 ± 20 fs. The FWHM of the probe pulse is 220 ± 20 fs as measured via the frequency-resolved optical gating technique.[36]

We measure the transient thermoreflectance signal on a thin Au film ($\sim$26 nm thickness measured via picosecond acoustics[20,37]) evaporated on a Si substrate with a pump fluence averaged over the Gaussian diameter of either 0.5 or 6.1 J m^{-2}. The pump pulse energies and fluences do not significantly modify the conduction band number density from d-band excitations, and in fact, we estimate that even with our maximum absorbed fluence, the conduction band number density will only be perturbed by $<2\%$.[38] This validates the use of the Drude-based thermoreflectance model[39] to directly relate the change in the reflectivity measured to the temperature changes. The absorption of the pump pulses by the sample surface leads to an increase in the internal energy of the electron system, which consequently transfers its energy to the lattice vibrations through electronic collisions.

As the experimentally measured e-p coupling factor takes into account the contributions from various scattering mechanisms such as electron-interface, electron-defect, and electron-electron scattering simultaneously with purely e-p scattering, we assign an "effective" e-p coupling factor (G_{eff}) to describe the volumetric rate of energy transfer from herein. In typical pump-probe analyses, the thermoreflectance signal is related to temperature change through an appropriate thermoreflectance model and subsequently compared to the TTM to determine a constant G_{eff} value, which effectively accounts for all the scattering mechanisms responsible for the thermoreflectance signal averaged over the temporal response. As previously mentioned, this approach does not consider any temperature dependency in G_{eff} during the energy transfer from the electronic system to the surrounding lattice. We use a nonlinear, thickness-dependent thermoreflectance model, which has been explained in detail in Ref. 19, to fit the TTM to the experimental data on the thin film Au sample. The form of the TTM used is given by the following two coupled differential equations,[19] $C_e(T_e)\partial T_e/\partial t = -G_{\text{eff}}(T_e - T_p) + S(t)$ and $C_p(T_p)\partial T_p/\partial t = G_{\text{eff}}(T_e - T_p)$. The electronic heat capacity is calculated using the *ab initio* DOS based on the procedure described by Lin *et al.*[26] The laser source term, $S(t)$, is given by $S(t) = (0.94(1-R)F/(d(t_p + \tau_F)))\exp[-2.77(t/(t_p + \tau_F))^2]$, where R is the reflectivity of the Au film, F is the incident fluence, d is the film thickness, t_p is the pump pulse width, and τ_F is the Fermi relaxation time of the excited electron system. The source term has been modified in order to account for the delayed thermalization of the electronic system in Au,[19] which in practice is determined by fitting the portion of the thermoreflectance data before the maximum signal.

Although the TTM in conjunction with the thermoreflectance model reproduces the literature values of e-p coupling factor, the constant G_{eff} assumption during and after laser absorption needs to be reconsidered. For example, in the regime of our experiments in this work, a change in absorbed fluence (and subsequent change in electron temperature) can lead to $\sim$50% change in G_{eff}.[23,32] From this, G_{eff} must depend on electron temperature, and therefore the traditional implementation of the TTM is incorrect to assume a constant G_{eff} over the picosecond decay after pulse absorption. Furthermore, given the large changes in the e-p coupling factor demonstrated in prior works when thermally exciting sub-Fermi surface bands,[23,26,40–42] assuming a constant G_{eff} in pump-probe experiments when considering electronic temperature excursions of several thousand Kelvin is clearly invalid.

To account for the transient e-p coupling factor during and after laser pulse absorption and simultaneously test the validity of the aforementioned models, we replace G_{eff} in the TTM with the temperature-dependent e-p coupling factors described above (Eqs. (1) and (5)) to reproduce the measured thermoreflectance signals. The best fits to the experimental data with the models are shown in Fig. 3. To this end, we

fit the TTM with Eq. (1) by treating A_{ee} and B_{ep} as free parameters. We find $A_{ee} = 1.3 \times 10^7\,\mathrm{K^{-2}\,s^{-1}}$ and $B_{ep} = 1.1 \times 10^{11}\,\mathrm{K^{-1}\,s^{-1}}$, which are in excellent agreement with literature values.[17,40] To calculate Eq. (5), we approximate the excited number density of electrons as $N_{ex} = F/h\nu\delta$, where $h\nu$ is the photon energy and δ is the optical penetration depth. The fraction of excited electron density, n_{ex}, is given by N_{ex}/N, where N is the conduction band density (since, in this study, our pump pulse energies will lead to a negligible perturbation in conduction band number density as discussed above, we take N as the conduction band density, $5.9 \times 10^{28}\,\mathrm{m^{-3}}$).

Figure 3 shows the results of the model fits to the thermoreflectance signals for high and low laser fluences. For the case of low electron temperatures ($T_{e,max} \sim 700\,\mathrm{K}$) resulting from the low absorbed laser fluence (see Fig. 3(a)), both Eqs. (1) and (5) replaced in the TTM can predict the thermoreflectance response reasonably well. However, for the case of high electron temperatures ($T_{e,max} \sim 2800\,\mathrm{K}$) resulting from the higher laser fluence, replacing Eq. (5) in the TTM grossly under-predicts the e-p coupling factor and therefore fails to reproduce the experimentally measured thermoreflectance signal. As mentioned earlier, the inclusion of nonthermal electrons losing energy to the lattice cannot significantly increase the e-p coupling factor to correctly predict the thermoreflectance signal at high fluences. It should be noted that even an increase in n_{ex} to more than 10% cannot account for the increase in the e-p coupling factor needed to reproduce the thermoreflectance signal. This suggests that along with thermal and nonthermal electron coupling to the phonons, there must be other energy relaxation mechanisms simultaneously increasing the rate of electron relaxation at these timescales after laser pulse absorption.

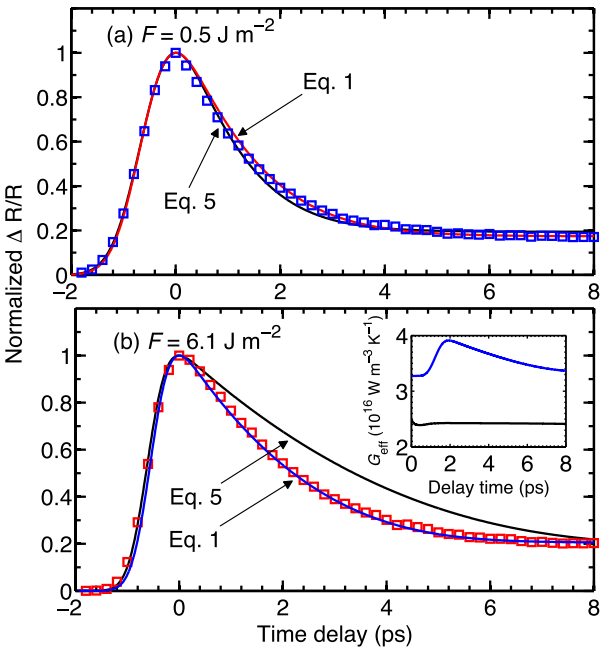

FIG. 3. TDTR data and the TTM fits for the data (solid lines) as a function of the delay time after pulse absorption for (a) $F = 0.5\,\mathrm{J\,m^{-2}}$ and (b) $F = 6.1\,\mathrm{J\,m^{-2}}$. For the low fluence case, replacing Eq. (1) or Eq. (5) in the TTM can reproduce the thermoreflectance signal. However, for the high fluence case, Eq. (5) in the TTM under-predicts the relaxation rates during electron-phonon nonequilibrium. Accounting for electron-electron scattering by replacing Eq. (1) in the TTM can correctly predict the thermoreflectance signal at these high electron temperatures.

To reproduce the thermoreflectance signal at high laser fluences (and high T_e), we replace G_{eff} in the TTM with Eq. (1) that accounts for the thermalized e-e scattering mechanisms along with e-p scattering in the e-p coupling factor. As shown in Fig. 3(b), the best fit to the thermoreflectance signal with the TTM based on Eq. (1) correctly predicts the experimental data at these high electron temperatures ($T_{e,max} \sim 2800\,\mathrm{K}$). This agreement demonstrates that along with strictly e-p scattering, e-e scattering in a thermalized electron system must be considered to correctly account for the high energy relaxation with the lattice during relatively high intensity laser excitation of metals. The importance of accounting for e-e scattering to correctly reproduce this transient nature of energy exchange rate is further exemplified in the inset of Fig. 3(b), where the effective e-p coupling factors predicted from Eqs. (1) and (5) are plotted as a function of delay time for the high fluence case. It should be noted that even though Eq. (5) depends on T_e, at high electron temperature perturbations, e-e scattering mechanisms dominate the energy relaxation processes and therefore have to be considered to correctly predict the dynamics of electron relaxation in laser heated metals. Note, the maximum in the reflectivity is observed at a longer delay time compared to the Fermi relaxation time period ($\sim$1 ps),[41] which suggests that the peak in the electronic temperature is reached at a later time after the electrons have thermalized. This could be understood as a consequence of increase in the phase space of electrons as the thermalization progresses, which eventually leads to higher e-e scattering and an increase in the rate of e-p relaxation (for which the maximum is observed at $\sim$2 ps after laser pulse absorption as shown in the inset of Fig. 3(b)). To further verify the claim that e-e scattering plays a major role at high T_e, we modify Eq. (1) to account for d-band electron excitation under intense laser heating, which perturbs electronic states to >4000 K, detailed in Sec. IV.

IV. HIGH TEMPERATURE TRANSIENT ELECTRON RELAXATION

A. EEET

To determine the electron-phonon coupling factor for high electron temperatures that can be achieved in, for example, thermionic emission and pulsed laser ablation experiments, we derive the EEET with a relaxation time approximation, which describes the change in electron internal energy as a function of time due to e-p scattering. We start with the Boltzmann transport equation for electrons in one dimension, given by[43,44]

$$\frac{\partial f}{\partial t} + v_z \frac{\partial f}{\partial z} + \frac{F_z}{m}\frac{\partial f}{\partial v_z} = \left(\frac{\partial f}{\partial t}\right)_c, \tag{6}$$

where f is the nonequilibrium electron distribution function, v_z is the electron velocity in the z-direction, F_z is the Lorentz force in the z-direction, and the term $(\partial f/\partial t)_c$ is the time rate of change of the nonequilibrium distribution function due to

e-e and e-p collisions. In this analysis, the z-direction is taken as perpendicular to an interface that provides resistance to heat flow (i.e., the cross plane direction). In the thin film limit, when the film thickness is less than the ballistic penetration depth, Eq. (6) reduces to[15]

$$\frac{\partial f}{\partial t} = \left(\frac{\partial f}{\partial t}\right)_c, \tag{7}$$

since spatial gradients in the film are negligible. Note, the ballistic penetration depth in gold has been measured to be ~100 nm (Ref. 7) and our experimental measurements are in the thin film region to simplify this analysis. A more rigorous analysis could solve Eq. (6) without making this assumption, but the procedure discussed in this paper would remain identical. With Eq. (7), the EEET,[15,45] which parallels the equation of phonon radiative transport (EPRT),[46] is given by

$$\frac{\partial U_\epsilon(t)}{\partial t} = \left(\frac{\partial U_\epsilon(t)}{\partial t}\right)_c, \tag{8}$$

where t is the time and $U_\epsilon(t)$ is the volumetric electron energy density per unit energy defined as

$$U_\epsilon(t) = \epsilon D(\epsilon) f(1-f), \tag{9}$$

where the factor of $(1-f)$ is included due to the fact that the energy transfer can only occur when there are empty states in the vicinity of occupied states. Thus, the quantity $U = \int_\epsilon \epsilon D(\epsilon) f(1-f)$ gives the total energy per unit volume of the electron system. For thermalized electron systems with the equilibrium Fermi Dirac distribution, f_{FD}, the equilibrium energy density per unit energy is determined from Eq. (9) as

$$U_\epsilon(t) = \epsilon D(\epsilon) f_{FD}(1-f_{FD}), \tag{10}$$

where $f_{FD} = f_{FD}(\epsilon, \mu(T_e), T_e)$ with $\mu(T_e)$ being the chemical potential which depends on the electron temperature, T_e.

To evaluate the internal energy of the electron system, the density of states must be determined. Due to the fact that we are interested in electron temperature excursions on the order of 10 000 K in the work in this section, an accurate DOS representation of the electronic band structure is crucial for describing the e-p thermophysics.[26,47,48] Therefore, we use the *ab initio* DOS calculated for Au published previously.[15]

Figure 4 shows the equilibrium energy density for Au at 6 different electron temperatures calculated with Eq. (10) using the *ab initio* DOS. At relatively low temperatures, below the onset of d-band excitations ($T_e \sim 3000$ K), the energy density profile is a Gaussian that is centered around the Fermi energy. As the electronic temperature increases, the influence of the d-band electronic population becomes pronounced with large spikes in the internal energy around 2 eV below the Fermi energy. In addition, as temperature is increased, the effects of electronic excitations from the inner nonconstant s-band DOS and the p-band become apparent by the variations in the internal energy at energies far above the Fermi energy. It is important to note that the absolute value of the internal energy is arbitrary since it is related to the

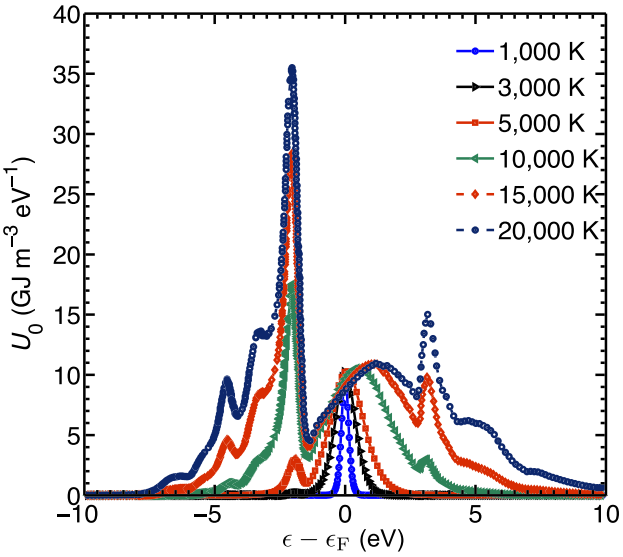

FIG. 4. Equilibrium energy density for Au at 6 different temperatures calculated with Eq. (10) using the *ab initio* density of states from Ref. 15. As the temperature is increased ($T_e > 3000$ K), the variation from the constant density of states around the Fermi energy becomes apparent with the onset of the d-band thermal excitations at ~2 eV below the Fermi energy and excitations of s- and p-band electrons at energies far above the Fermi energy.

energy of the electrons (i.e., $U_{\epsilon,0} \propto \epsilon$) which is dependent on the DOS calculations. For example, the Fermi energy of Au amounts to 16.25 eV from DOS calculations since both the $6s^1$ and $5d^{10}$ bands are accounted for in the calculation, whereas the Fermi energy is 5.53 eV if only conduction electrons are included in the calculation.

Evaluating the collision term on the right hand side of Eq. (8) gives the change in energy density with time due to e-p collisions. A relaxation time approximation (RTA) can be assumed to evaluate the electron energy density, which takes the standard form

$$\left[\frac{U_\epsilon}{\partial t}\right]_{ep} = \frac{U(t) - U_0(T_p)}{\tau_{ep}}. \tag{11}$$

Equation (11) is solved by recognizing that $U(t=0) = U_0(T_e)$, such that the rate of change of the total electron energy density is given by

$$U_{RTA}(t) = U_0(T_p) + (U_0(T_e) - U_0(T_p))\exp(-t/\tau_{ep}). \tag{12}$$

It should be noted that this derivation does not incorporate the e-p coupling factor, just a relaxation time is included, which represents how long the electrons at some elevated energy take to reach thermal equilibrium with the phonons.

B. General model for electron-phonon coupling

In Sec. IV A we derived a simple energy relaxation relationship for the transient decay of internal energy of an excited electron system. The utility in that derivation is the ability to relate the relaxation of the electrons to an intrinsic thermodynamic property of the system, i.e., U_ϵ. In this subsection, we review the quantum mechanical derivation of the

e-p coupling factor of a metal, G, and relate this to the EEET discussion in Sec. IV A.

Allen's model for the e-p coupling factor is derived from the standard Bloch-Boltzmann-Peierls formulas[49] for the rates of change of electron and phonon distributions[27]

$$\left[\frac{\partial f_k}{\partial t}\right]_{ep} = -\frac{2\pi}{\hbar}\sum_q |M_{kk'}|^2 f_k(1-f_{k'})[(N_q+1)\delta \times (\epsilon_k-\epsilon_{k'}-\hbar\omega_q)+N_q\delta(\epsilon_k-\epsilon_{k'}+\hbar\omega_q)] - (1-f_k)f_{k'}[(N_q+1)\delta(\epsilon_k-\epsilon_{k'}+\hbar\omega_q) + (N_q+1)\delta(\epsilon_k-\epsilon_{k'}-\hbar\omega_q)], \quad (13)$$

$$\left[\frac{\partial N_q}{\partial t}\right]_{ep} = -\frac{4\pi}{\hbar}\sum_k |M_{kk'}|^2 f_k(1-f_{k'})[N_q\delta(\epsilon_k-\epsilon_{k'}+\hbar\omega_q) - (N_q+1)\delta(\epsilon_k-\epsilon_{k'}-\hbar\omega_q)], \quad (14)$$

where M is the e-p scattering matrix element, N is the phonon distribution, ω is the phonon angular frequency, and k and q are the electron and phonon wavevectors, respectively. The rate of energy exchange between the electrons and phonons within one unit cell is given by

$$\left[\frac{\partial U}{\partial t}\right]_{ep} = -\frac{4\pi}{\hbar}\sum_{kk'} |M_{kk'}|^2 S(k,k')\delta(\epsilon_k-\epsilon_{k'}+\hbar\omega_q), \quad (15)$$

where S is the thermal factor that expresses the phonon absorption and emission processes during e-p scattering in terms of the electron and phonon occupation numbers. This thermal factor is given by

$$S(k,k') = (f_k - f_{k'})N_q - f_{k'}(1-f_k). \quad (16)$$

Given the Elaishberg spectral function for e-p coupling as a function of energy, which Wang *et al*. defines as[40]

$$\alpha^2(\epsilon_k,\epsilon_{k'})F(\omega_q) = [D(\epsilon_k)D(\epsilon_{k'}/(D(\epsilon_F))^2)]\alpha^2F(\omega_q), \quad (17)$$

where $\alpha^2F(\omega_q)$ is related to the e-p material properties through $\lambda\langle\omega^2\rangle = 2\int_0^\infty \omega_q\alpha^2F(\omega_q)\mathrm{d}\omega_q$, Eq. (15) can be rewritten as[27]

$$\left[\frac{\partial U}{\partial t}\right]_{ep} = 2\pi D(\epsilon_F)\int_0^\infty \hbar\omega_q\mathrm{d}\omega_q\int_0^\infty \mathrm{d}\epsilon_k \times \int_0^\infty \alpha^2F(\omega_q)S(\epsilon,\epsilon_{k'})\delta(\epsilon-\epsilon_{k'}+\hbar\omega_q)\mathrm{d}k. \quad (18)$$

For this derivation, we consider the electron and phonon systems to be completely thermalized at different temperatures before the majority of the e-p energy exchange takes place, such that f and N represent the Fermi-Dirac and Bose-Einstein distribution functions, respectively. This is a valid assumption for high laser fluences and electron temperatures ($T_e > 7000$ K)[41] as we have shown with the calculations of the electron distribution function in Section II.

After some algebra as described in detail in the Appendix of Ref. 26, the time rate of change of the electron energy due to e-p collisions is given by

$$\left[\frac{\partial U}{\partial t}\right]_{ep} = \pi\hbar k_B(T_p-T_e)\lambda\langle\omega^2\rangle\int_0^\infty \frac{(D(\epsilon))^2}{D(\epsilon_F)}\left[-\frac{\partial f_{FD}}{\partial\epsilon}\right]\mathrm{d}\epsilon, \quad (19)$$

where the e-p coupling factor is given by Eq. (2). We note that in the derivation of Eq. (2), fully thermalized electron and phonon systems are assumed, and electron relaxation with the lattice is assumed to be facilitated via only e-p scattering. These assumptions limit the application of this quantum mechanical approach, as we have described in detail in Sec. III.

It is convenient to use EEET described in the previous subsection (Sec. IV A) since we can relate the rate of change in the internal energy of the electron system to the e-p coupling factor by

$$\left[\frac{\partial U}{\partial t}\right]_{ep} = G(T_p - T_e). \quad (20)$$

To calculate G, we must determine the internal energy relaxation rate at a given temperature, or determine the transient temperature change given a known energy relaxation rate. Since the volumetric rate of energy relaxation in an electronic system is $C_e(T_e)\partial T_e/\partial t$ (which assumes a Fermi Dirac distribution for the electrons), for high electron temperatures $T_e \gg T_p$, we can express Eq. (20) as

$$G_{eff}(T_e) = -\frac{C_e(T_e(t))}{T_e(t)}\frac{\partial T_e(t)}{\partial t}. \quad (21)$$

For low temperature perturbations and when electronic and vibrational systems are in equilibrium ($T_p = T_e$), Eq. (20) suggests that the internal energy of the electron system does not change due to e-p scattering events. In other words, Eq. (20) implies that when electrons equilibrate with the phonons, there is no resistance to electrons in metals due to e-p collisions. Therefore, Eqs. (20) and (21) do not account for finite e-p resistance when gradients in temperature are present in the regime when $T_p \sim T_e$ (i.e., thermal diffusion) as in the experiments. Thus, we modify Eq. (21) to account for conditions of relatively minor nonequilibrium between the electrons and phonons and assume

$$G_{eff}(T_e) = -\frac{C_e(T_e(t))}{T_e(t)}\frac{\partial T_e(t)}{\partial t} + G_0. \quad (22)$$

Equation (22) is consistent with Kaganov's original expression[12,25] and Allen's derivation of the e-p thermal relaxation.[27] Given the transient electron temperature that is obtained from pump-probe thermoreflectance data (which relates the reflectivity of the sample surface to the transient temperature change), the effective e-p coupling factor can be determined through Eq. (22). Note, we use the term "effective" to describe the e-p coupling factor in Eq. (22) as the pump-probe experiments take into account various scattering mechanisms other than purely e-p scattering. In Sec. IV C, we will apply Eq. (22) to analyze previously reported experimental data to evaluate the role of e-e scattering on overall e-p relaxation at high temperatures during d-band excitation in gold.

C. Electron-phonon coupling at high electron temperatures

To investigate the e-p dynamics at high electron temperatures and e-p nonequilibrium, we modify the model of Chen

et al.[24] to account for the d-band thermal excitation. At high e-p nonequilibrium, thermal excitations from the d-band will affect the various scattering mechanisms, which can lead to faster electronic relaxations as demonstrated by the model of Lin *et al.*[26] Therefore, in this section, we modify Eq. (1) to account for changes in e-e and e-p scattering due to d-band excitations at high temperatures.

We start with the expression derived by Kaganov for the rate of energy transfer between electrons and the lattice, which considers all one-phonon emission and absorption processes[25]

$$\left[\frac{\partial U}{\partial t}\right]_{ep} = \frac{2}{(2\pi)^3}\frac{m^2U^2(k_BT_D)^5}{\hbar^7\rho v_s^4}\left\{\left(\frac{T_e}{T_D}\right)^5\int_0^{T_D/T_e}\frac{x^4}{e^x-1}dx - \left(\frac{T_p}{T_D}\right)^5\int_0^{T_D/T_p}\frac{x^4}{e^x-1}dx\right\}, \quad (23)$$

where ρ is the mass density. In the limiting case of high temperatures T_e, $T_p \gg T_D$, Eq. (22) can be expressed as

$$\left[\frac{\partial U}{\partial t}\right]_{ep} = \frac{\pi^2 n_e m v_s^2}{6}\left\{\frac{1}{\tau_e(T_e)} - \frac{1}{\tau_e(T_p)}\right\}, \quad (24)$$

where $\tau_e(T_e)$ and $\tau_e(T_p)$ are the time of free flight of electrons at the electronic and lattice temperatures, respectively. In deriving the general form of energy exchange given in Eq. (1), Chen *et al.* considered both e-e and e-p scatterings events to calculate the electron collision frequency, $\tau_{e-e} = (\nu_{e-e} + \nu_{e-p})^{-1}$, where ν_{e-e} and ν_{e-e} represent the e-e and e-p collision rates.[24] For high temperatures ($T_p > T_D$) but in the limit of electron energy that is less than the Fermi energy, $\nu_{e-e} = \nu_{e0}\,(T_F/T_e)^2$ and $\nu_{e-p} = \nu_{p0}\,(T_F/T_p)$, where ν_{e0} and ν_{p0} are material constants. Therefore, $\tau_e(T_e, T_p) = (A_{ee}T_e^2 + B_{ep}T_p)^{-1}$, where the material constants, $A_{ee} = (\nu_{e0}T_F^2)^{-1}$ and $B_{ep} = (\nu_{p0}T_F)^{-1}$ are generally determined at low temperatures as discussed in Section III.[9,40,50]

Replacing $\tau_e(T_e, T_p)$ in Eq. (24), we get the general expression for the rate of energy exchange between electrons and the lattice that is applicable at high temperatures[24]

$$\left[\frac{\partial U}{\partial t}\right]_{ep} = \frac{\pi^2 n_e m v_s^2}{6}[A_{ee}(T_e + T_p) + B_{ep}](T_e - T_p). \quad (25)$$

Thus, the temperature-dependent e-p coupling factor described in Eq. (1) is obtained from the above expression. However, the use of constant A_{ee} and B_{ep} (that are determined at low temperatures) in Eq. (1) may not be applicable to situations where a significant portion of d-band electrons are perturbed, which renders A_{ee} and B_{ep} to be dependent on electron temperature. Therefore, we modify Chen's expression for the e-p coupling factor to accommodate for the temperature dependency of these scattering constants to extend this model to free-electron metals with arbitrary density of states

$$G_{eff} = \frac{\pi^2 m v_s^2 n_e}{6}\left[A_{ee}(T_e)(T_e + T_p) + B_{ep}(T_e)\right]. \quad (26)$$

The electron temperature dependence of the scattering coefficients is estimated with an approach similar to that discussed by Chan *et al.*[51] The temperature dependency of B_{ep} is assumed to take the form

$$B_{ep}(T_e) \approx B_{ep,0}(1 + C_{ep}n_d(T_e)), \quad (27)$$

where $B_{ep,0}(\sim 1.1\times10^{11}\,s^{-1}\,K^{-1})$ is the low temperature value that we determined from fitting of the thermoreflectance data in Sec. III and C_{ep} represents the ratio of the d-band e-p coupling to the s-band e-p coupling; n_d is the number density of the other electronic bands away from the Fermi level. For Au, n_d is the number density of the $5d^{10}$ bands that are thermally excited per atom. This is calculated by $n_d(T_e) = \int_\epsilon D_d(\epsilon)(1-f)d\epsilon$, where D_d is the density of states of the d-bands, which is obtained from the *ab initio* density of states calculations for Au.[15] Similarly, for $A_{ee}(T_e)$, we use the expression by Chan *et al.*,[51] and since the number of d-band electrons thermally excited to the s-band is identical to the number of d-band holes excited in the d-band

$$A_{ee}(T_e) \approx A_{ee,0}(1 + C_{ee}n_d(T_e)), \quad (28)$$

where $A_{ee,0d}$ $(\sim 1.3\times10^7\,s^{-1}\,K^{-2})$ is the low temperature value that we determined from the thermoreflectance fitting described in the earlier section. Chan *et al.*[51] estimates C_{ee}, the corresponding ratio of e-e scattering, as $C_{ee} = 150$ based on the ratio of $A_{ee,0}$ for Ni to free electron metals. The reasoning behind using $A_{ee,0}$ for Ni is because it has d-bands overlapping the Fermi level so that the low temperature e-e scattering coefficient in Ni is dominated by d-band hole scattering where the coefficients in free electron metals are dominated by the s-band electron scattering. Using this same approach for B_{ep}, we determine $C_{ep} = 200$. We assume that the effective mass, m, is constant in Eq. (26) since we are interested in Au in this study, and therefore the e-p scattering will be dominated by electrons excited into the s-band.

At relatively high electronic temperatures of ~10 000 K for Au, the contribution from d-band electrons to the total number density of excited electrons is ~8%. However, Eqs. (27) and (28) predict a relatively large change in the scattering coefficients B_{ep} and A_{ee} compared to the constant, low temperature-determined scattering coefficients (by ~18 and ~14 folds, respectively) due to d-band excitation at $T_e \sim 10\,000$ K. Therefore, G_{eff} predicted by Eq. (26) with the temperature-dependent scattering coefficients increases by more than 15-fold compared to the prediction from Eq. (1), with constant scattering coefficients at these relatively high temperatures. As apparent from the discussion above, this large change in G_{eff} at high electron temperatures is due to the increased scattering rates of the excited electrons, while the increase in electron number density on the Fermi surface has a relatively negligible effect. Therefore, for the purpose of Eq. (26), it is acceptable to assume that n_e is constant. While this assumption is valid for Au, and other free electron metals, we caution that this model may not be applicable for transition metals with a large variation in the electronic density of states around the Fermi energy.

Figure 5 shows the calculations of Eq. (26) along with the predictions of Eq. (1) (the model of Chen *et al.*)[24] and Eq. (2) (the model of Lin *et al.*)[26] for Au. As mentioned

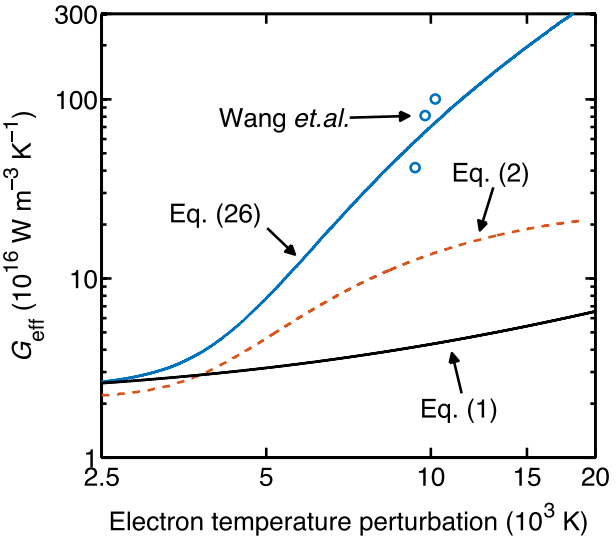

FIG. 5. Various models for the e-p coupling factor discussed in the text as a function of electron temperature perturbation. Also included are experimental data from Ref. 40 at high electron temperatures. The agreement between the high temperature experimental data and our model in Eq. (26) represents the significance of accounting for e-e scattering and d-band excitations in determining G_{eff}.

above, at higher temperatures, when d-band electrons are excited near the Fermi surface, Eq. (26) predicts a larger increase in the effective e-p coupling factor beyond the prediction from Eqs. (1) and (2). This is due to the fact that G_{eff} in Eq. (26) takes into account e-e scattering as per the model of Chen *et al.*[24] and also considers scattering due to d-band electrons and holes. The TTM approach cannot be used to determine G_{eff} since the e-p coupling is clearly nonlinear (from the model of Lin *et al.*),[26] and therefore RTA solutions to energy decay break down. However, Eq. (22) is still valid and to test Eq. (22) at high electron temperatures, we apply it to the electron temperature ($\sim$0.94 eV) temporal profile measured by Wang *et al.*[40] We only apply Eq. (22) to three data points after the peak temperature of Fig. 2 in Ref. 40 to avoid any substantial lattice heating. G_{eff} as a function of temperature from the data of Wang *et al.* are plotted in Fig. 5 (hollow circles) and show good agreement with the prediction of Eq. (26). This indicates the importance of accounting for e-e scattering that considers the d-band electrons in interpretation of high temperature electron relaxation data, since this substantially contributes to the overall e-p equilibration process. It should be noted that due to the large increase in electron relaxation when d-band electrons and holes are excited near the Fermi surface and electrons thermalize at a much faster rate, it is expected that even if the high temperature measurements were taken on thinner films, the effects of the d-band excitations on electron relaxation would far outweigh the potential effects of electron boundary scattering.

V. SUMMARY

In summary, we have studied the temperature dependency of electron relaxation after short-pulsed laser absorption that creates nonequilibrium within and between the electronic and the vibrational states. An analytical expression is derived for the electron-phonon coupling factor in a metal with a nonthermal electron distribution. In the low perturbative regime, the nonthermal electron gas can still interact with the phonon system but at a much slower rate than the corresponding thermalized electron distribution. As a consequence, the interaction of nonthermal electrons with the surrounding lattice can lead to the transient behavior of the electron-phonon relaxation rate, contrary to the monotonous nature of coupling demonstrated by the thermalized distribution at low electron perturbations. However, even with the inclusion of nonthermal electron-phonon coupling in the general expression for the electron-phonon coupling factor, the high rates of energy transfer measured by thermomodulation techniques for high absorbed laser fluences cannot be predicted by these models. We have attributed this disagreement to the fact that these analytical models do not account for electron-electron scattering, a process which is present during relaxation of a short-pulsed excited electronic system with a thermalized phonon system in a metal. Consequently, by comparing the experimentally measured thermoreflectance responses of a thin Au film at different laser fluences to the two-temperature model based on the various electron-phonon coupling models, we demonstrated that not accounting for electron-electron scattering can significantly under-predict the electron relaxation rates at elevated electron perturbations. Furthermore, for electron temperatures $>$3000 K, we derive a procedure that accounts for electron-electron and electron-phonon scattering during electron-phonon thermalization using an *ab initio* electronic density of states to properly account for the shape of the $5d^{10}$ bands in Au. By accounting for d-band excitations at high electron perturbations, we show good agreement between our analytical model with previous experimental data, further demonstrating the role of electron-electron scattering during electron-phonon relaxation under conditions of strong nonequilibrium.

ACKNOWLEDGMENTS

This material is based upon work supported by the Air Force Office of Scientific Research under AFOSR Award No. FA9550-15-1-0079.

[1]A. Majumdar, K. Fushinobu, and K. Hijikata, J. Appl. Phys. **77**, 6686 (1995).
[2]C.-K. Sun, F. Vallée, L. Acioli, E. P. Ippen, and J. G. Fujimoto, Phys. Rev. B **48**, 12365 (1993).
[3]C.-K. Sun, F. Vallée, L. H. Acioli, E. P. Ippen, and J. G. Fujimoto, Phys. Rev. B **50**, 15337 (1994).
[4]W. S. Fann, R. Storz, H. W. K. Tom, and J. Bokor, Phys. Rev. Lett. **68**, 2834 (1992).
[5]S. D. Brorson, J. G. Fujimoto, and E. P. Ippen, Phys. Rev. Lett. **59**, 1962 (1987).
[6]S. D. Brorson, A. Kazeroonian, J. S. Moodera, D. W. Face, T. K. Cheng, E. P. Ippen, M. S. Dresselhaus, and G. Dresselhaus, Phys. Rev. Lett. **64**, 2172 (1990).
[7]J. Hohlfeld, S.-S. Wellershoff, J. Güdde, U. Conrad, V. Jähnke, and E. Matthias, Chem. Phys. **251**, 237 (2000).
[8]P. E. Hopkins, J. L. Kassebaum, and P. M. Norris, J. Appl. Phys. **105**, 023710 (2009).
[9]P. E. Hopkins, J. C. Duda, B. Kaehr, X. W. Zhou, C.-Y. P. Yang, and R. E. Jones, Appl. Phys. Lett. **103**, 211910 (2013).
[10]P. E. Hopkins, J. Appl. Phys. **106**, 013528 (2009).
[11]G. Della Valle, M. Conforti, S. Longhi, G. Cerullo, and D. Brida, Phys. Rev. B **86**, 155139 (2012).

[12]S. I. Anisimov, B. L. Kapeliovich, and T. L. Perelman, Sov. Phys. JETP **39**, 375 (1974).
[13]K.-H. Lin and A. Strachan, J. Chem. Phys. **143**, 034703 (2015).
[14]S. Sadasivam, U. V. Waghmare, and T. S. Fisher, J. Appl. Phys. **117**, 134502 (2015).
[15]P. E. Hopkins and D. A. Stewart, J. Appl. Phys. **106**, 053512 (2009).
[16]Y. Wang, X. Ruan, and A. K. Roy, Phys. Rev. B **85**, 205311 (2012).
[17]D. S. Ivanov and L. V. Zhigilei, Phys. Rev. B **68**, 064114 (2003).
[18]W. S. Fann, R. Storz, H. W. K. Tom, and J. Bokor, Phys. Rev. B **46**, 13592 (1992).
[19]P. E. Hopkins, L. M. Phinney, and J. R. Serrano, J. Heat Transfer **133**, 044505 (2011).
[20]G. Tas and H. J. Maris, Phys. Rev. B **49**, 15046 (1994).
[21]R. H. M. Groeneveld, R. Sprik, and A. Lagendijk, Phys. Rev. B **45**, 5079 (1992).
[22]R. H. M. Groeneveld, R. Sprik, and A. Lagendijk, Phys. Rev. B **51**, 11433 (1995).
[23]A. Giri, J. T. Gaskins, B. M. Foley, R. Cheaito, and P. E. Hopkins, J. Appl. Phys. **117**, 044305 (2015).
[24]J. K. Chen, W. P. Latham, and J. E. Beraun, J. Laser Appl. **17**, 63 (2005).
[25]M. Kaganov, I. Lifshitz, and L. V. Tanatarov, Sov. Phys. JETP **4**, 173 (1957).
[26]Z. Lin, L. V. Zhigilei, and V. Celli, Phys. Rev. B **77**, 075133 (2008).
[27]P. B. Allen, Phys. Rev. Lett. **59**, 1460 (1987).
[28]E. Carpene, Phys. Rev. B **74**, 024301 (2006).
[29]G. D. Tsibidis, Appl. Phys. Lett. **104**, 051603 (2014).
[30]D. Pines and P. Nozières, *The Theory of Quantum Liquids* (Benjamin, 1966).
[31]C. Kittel, *Introduction to Solid State Physics*, 6th ed. (John Wiley & Sons, Inc., New York, 1986).
[32]P. E. Hopkins, ISRN Mech. Eng. **2013**, 682586.
[33]D. G. Cahill, Rev. Sci. Instrum. **75**, 5119 (2004).
[34]A. J. Schmidt, X. Chen, and G. Chen, Rev. Sci. Instrum. **79**, 114902 (2008).
[35]P. E. Hopkins, J. R. Serrano, L. M. Phinney, S. P. Kearney, T. W. Grasser, and C. T. Harris, J. Heat Transfer **132**, 081302 (2010).
[36]R. Trebino, K. W. DeLong, D. N. Fittinghoff, J. N. Sweetser, M. A. Krumbügel, B. A. Richman, and D. J. Kane, Rev. Sci. Instrum. **68**, 3277 (1997).
[37]C. Thomsen, H. T. Grahn, H. J. Maris, and J. Tauc, Phys. Rev. B **34**, 4129 (1986).
[38]P. E. Hopkins, T. E. Beechem, J. C. Duda, J. L. Smoyer, and P. M. Norris, Appl. Phys. Lett. **96**, 011907 (2010).
[39]A. N. Smith and P. M. Norris, Appl. Phys. Lett. **78**, 1240 (2001).
[40]X. Y. Wang, D. M. Riffe, Y.-S. Lee, and M. C. Downer, Phys. Rev. B **50**, 8016 (1994).
[41]B. Y. Mueller and B. Rethfeld, Phys. Rev. B **87**, 035139 (2013).
[42]B. Mueller and B. Rethfeld, Appl. Surf. Sci. **302**, 24–28 (2014).
[43]J. Chen, D. Tzou, and J. Beraun, Int. J. Heat Mass Transfer **49**, 307 (2006).
[44]T. Q. Qiu and C. L. Tien, J. Heat Transfer **115**, 842 (1993).
[45]P. E. Hopkins and P. M. Norris, J. Heat Transfer **131**, 043208 (2009).
[46]A. Majumdar, J. Heat Transfer **115**, 7 (1993).
[47]P. E. Hopkins, J. C. Duda, R. N. Salaway, J. L. Smoyer, and P. M. Norris, Nanoscale Microscale Thermophys. Eng. **12**, 320 (2008).
[48]Z. Lin and L. V. Zhigilei, Appl. Surf. Sci. **253**, 6295 (2007).
[49]J. M. Ziman, *Electrons and Phonons* (Clarendon Press, Oxford, 1960).
[50]M. Kaveh and N. Wiser, Adv. Phys. **33**, 257 (1984).
[51]W.-L. Chan, R. S. Averback, D. G. Cahill, and A. Lagoutchev, Phys. Rev. B **78**, 214107 (2008).